

Roles of SiH₄ in growth, structural changes and optical properties of nanocrystalline silicon thin films

メタデータ	言語: eng 出版者: 公開日: 2022-01-24 キーワード (Ja): キーワード (En): 作成者: メールアドレス: 所属:
URL	https://doi.org/10.24517/00064710

This work is licensed under a Creative Commons Attribution-NonCommercial-ShareAlike 3.0 International License.



Roles of SiH₄ in Growth, Structural Changes and Optical Properties Of Nanocrystalline Silicon Thin Films

Cite as: AIP Conference Proceedings **1370**, 68 (2011); <https://doi.org/10.1063/1.3638084>
Published Online: 28 October 2011

A. M. Ali, T. Inokuma, A. Al-Hajry, et al.



View Online



Export Citation

ARTICLES YOU MAY BE INTERESTED IN

[Electron Impact Dissociation of Molecular Ions for Thermonuclear Plasmas](#)

AIP Conference Proceedings **1370**, 33 (2011); <https://doi.org/10.1063/1.3638079>

[Solution of the Dirac equation in a one-dimensional box](#)

AIP Conference Proceedings **1370**, 21 (2011); <https://doi.org/10.1063/1.3638077>

[Study on Mössbauer and Magnetic Properties of Strontium–Neodymium Ferrimanganites Perovskite-Like Structure](#)

AIP Conference Proceedings **1370**, 103 (2011); <https://doi.org/10.1063/1.3638089>

LEARN MORE



Author Services

Maximize your publication potential with
English language editing and
translation services



Roles of SiH₄ in Growth, Structural Changes and Optical Properties Of Nanocrystalline Silicon Thin Films

A. M. Ali^{a,b,*}, T. Inokuma^c, A. Al-Hajry^d, H. Kobayashi^e, I. Umezu^f
and A. Morimoto^c

^aPhysics Department, Faculty of Science, King Khalid University, Abha, Saudi Arabia

^bPhysics Department, Faculty of Science, Assiut University, Assiut 71516, Egypt

^cGraduate School of Natural Science and Technology, Kanazawa University, Japan

^dPhysics Department, Faculty of Science, Najran University, Saudi Arabia

^eInstitute of Scientific and Industrial Research, Osaka University, Japan

^fPhysics Department, Faculty of Science, Konan University, Japan

E-mail: atifmossadali@yahoo.com

Abstract: Nanocrystalline silicon (ns-Si) thin films deposited through plasma-enhanced chemical vapor deposition technique were studied. These films were grown at low deposition temperature of 200 °C and at different silane flow rates ([SiH₄]). Characterization of these films with Raman spectroscopy, x-ray diffraction and atomic force microscopy revealed that no films deposited at [SiH₄] = 0.0 sccm. In addition, the structural change from an amorphous to a nanocrystalline phase at [SiH₄] = 0.2 sccm. The Fourier transform infrared spectroscopic analysis showed at low values of [SiH₄] (0.1 sccm), no hydrogen incorporated in the nc-Si thin film. However, the intensity of the spectra around 2100 cm⁻¹ is likely to decrease with increasing [SiH₄]. We have observed photoluminescence (PL) at room temperature in the range of 1.7 eV to 2.4 eV for all the films. Presence of the very small crystallites (the size less than 20 nm) responsible for quantum confinement effect. Variations of the PL intensity, width and position are well correlation with the structural properties of the films such as crystalline size, crystalline volume fraction, and hydrogen content. Furthermore, the PL emissions also showed correlation with the distribution of spherical grains with the size below 50 nm distributed on the films surface.

Keywords: Nanocrystalline silicon; PECVD; Photoluminescence; Quantum-size effect.

PACS: 81.07.Bc; 68.55._a; 78.55.Ap; 78.66.Li; 81.15.Gh; 81.10.Bk

INTRODUCTION

Since the discovery of room temperature (RT) photoluminescence (PL) in the visible range from porous silicon research efforts on the creation of nanostructured silicon is the mainstream of modern nanoelectronics and optoelectronics, because of its unique properties associated with the quantum confinement [1]. Among the various structures and approaches, nanocrystalline silicon (nc-Si) thin films have received great attention for their potential application in various devices, for example solar cells, and thin film transistors in liquid crystal displays, compared to amorphous silicon (a-Si) thin films along with better stability [2]. In particular, it is expected that this material can be used to fabricate Si-based optoelectronic devices in near future [3]. Recently, it has been known that quantum size effects of Si nanocrystallites are the main source for the unique and useful features of the materials and devices; these include a blue shift of the optical band [4], and visible PL [5].

Si nanocrystals produced with two different techniques, one is the re-crystallization of a-Si films as indirect technique, and the other is direct deposition. The recrystallization technique includes rapid thermal annealing (RTA) [6], laser-melt re-crystallization (LMR) [7] and aluminium-induced crystallization [8]. However, these methods have

difficulties in accurate control of crystallite size and crystalline fraction. In addition, post annealing at temperatures over 1000 °C is generally required for the crystallization of Si nanoparticles. Such high annealing temperature inevitably limits its further applications in optoelectronic devices. On the other hand, a variety of direct chemical vapor deposition (CVD) techniques have been used to yield material with good optoelectronic properties. These include plasma enhanced CVD (PE-CVD) [9-14] and its variant very high frequency glow discharge (VHF-GD) [15,16]. Other CVD methods employed in the deposition of nc-Si are electron cyclotron resonance-CVD (ECR-CVD) [17], homo-CVD [18], low energy P-CVD [19,20], low-pressure chemical vapor deposition (LPCVD) [21] and hotwire-CVD (HW-CVD) [22]. Among these, The PECVD technique appears to be a promising deposition method for large-area thin film technology and has been employed for industrial applications [23].

Deposition conditions play an important role in the growth of the nc-Si film, because it can affect the selective etching, the chemical etching and the thermal kinetic process of the film growth. Moreover, a low processing temperature can enlarge the application field of nc-Si film in wider industrial production by using low-cost substrate. Therefore, how to lower the processing temperature is becoming a challenging task for the semiconductor research community.

Several growth processes based on PECVD technique have been studied for the production of nc-Si which exhibits PL even at room temperature (RT) [24-28]. Although there is a large amount of research in the recent years, the mechanism underlying the visible luminescence is still unclear. There are two mechanisms, first one is the quantum confinement model and the second is the surface model, widely discussed to know the origin of PL. Fabrication of nc-Si films, having a highly efficient quantum-size effect, requires both a reduction in the grain size, δ , and an enhancement in the crystalline volume fraction, p . Then, an increase in the nucleation rate would become a key technique to be developed. It has been reported that the enhanced nucleation on the growing surface during deposition of nc-Si can be achieved by increasing the hydrogen flow rate, $[H_2]$ [29,30], or the deposition temperature, T_d [31]. However, the increase in T_d also caused an increase in δ . Thus, the increase in $[H_2]$ leads to reduction of δ [29, 30], while the increase in T_d should lead to increase in δ [31]. Furthermore, it has been reported that formation of nc-Si is due also to higher etching activity of hydrogen radicals for the amorphous phase than the crystalline one [32,33].

In order to contribute such device development, nc-Si films were deposited by PECVD. In general, this material could be described as a biphasic material consisting of nanocrystalline grains dispersed in a-Si matrix, with the grain boundaries acting as potential barriers for the carriers. Thus, grain size and its distribution affect the properties of these nc-Si films and make their study interesting. Efforts to understand the growth processes in nc-Si have been carried out by many researchers [34–37]. However, the mechanism is not fully understood because of the complex structure of these films. The purpose of this work is to investigate the effect of the SiH_4 on the grain size and optical properties of nc-Si films and to analyze luminescence spectra, and study the origin of PL in nc-Si films.

EXPERIMENTAL DETAILS

Nc-Si films were deposited on glass (Corning 7059) and fused quartz substrates by PECVD using a $SiH_4/SiF_4/H_2$ gas mixture. The remarkable feature of this deposition system is that the samples are exposed to the plasma (the growing surface is bombarded with ions). Just prior to the deposition of nc-Si films, the substrates were sequentially cleaned by rinsing them for 30 min in acetone and then in ethyl alcohol using an ultrasonic syringe. The samples were more cleaned by exposing them to N_2 and then to H_2 plasma at 90 W for 20 min just before the deposition of nc-Si films. The samples were deposited on 0.3-mm-thick glass (Corning 7059) substrates with an area of 10 x 20 mm² for measurements of X-ray diffraction (XRD), Raman scattering and atomic force microscopy (AFM), on 0.3-mm-thick fused quartz substrates with an area of 10 x 20 mm² for measurements of PL and optical absorption.

The rf power supply and the deposition temperature during the film deposition were maintained at 30 W and 200 °C, respectively. The feed gases were $SiF_4/SiH_4/H_2$ with the flow rates of $[SiF_4] = 0.2$ sccm, $[H_2] = 15$ sccm and $[SiH_4]$ was varied from 0 – 0.7 sccm.

The structural properties of the nc-Si films were investigated by means of XRD (SHIMADZU XD-D1) employing a diffractometer with the slit width of 0.1 mm, set at the front of the detector. The relative intensity (integrated area) of the XRD spectra from different crystal planes in the nc-Si was normalized by the corresponding x-ray intensity for Si powder.

The crystallinity was also characterized by Raman scattering measurements. The Raman spectra consisted of a narrow line at 520 cm⁻¹ due to a crystalline phase (c-phase) and a broad line around 480 cm⁻¹ due to an amorphous phase (a-phase). Since the third component between 480 and 520 cm⁻¹ due to very small crystallites was relatively

weak. Further, the surface morphology of the films was investigated by means of AFM (Park scientific instruments, AUTOPROBE GP/M5).

PL was analyzed using a Jobin Yvon RAMANOR HG 2S spectrometer coupled with a cold photo-multiplier tube (Hamamatsu Photonics R649S). The 488 nm Ar-ion laser with power 40 mW was used as the PL excitation source.

RESULTS AND DISCUSSION

In order to further improve properties of nc-Si thin films and performances of related devices, it is necessary to understand microstructure features of the films in detail. As a powerful technique, Raman spectroscopy has been extensively adopted to investigate the low-dimension structure materials because it is convenient and inexpensive and does not damage samples [38]. Moreover, Raman spectroscopy is useful for nondestructive characterization of stress and defects in nc-Si thin films. The Si optical phonon mode exhibits a line at around 520 cm^{-1} in the Raman spectra. Its peak frequency and full width at half-maximum are sensitive to stress, defect and grain size, δ . Figure 1 shows a typical Raman spectra from nc-Si thin films deposited at different $[\text{SiH}_4]$, which can be identified as two regions corresponding to two kinds of phonon modes, i.e., a transverse optical (TO1) branch with a peak at 480 cm^{-1} from the a-Si contribution and another transverse optical (TO2) mode at around 520 cm^{-1} from the contribution of Si nanocrystals, as mentioned before. As revealed in this diagram, the films with $[\text{SiH}_4]$ higher than 0.1 sccm exhibit a narrow peak at around 520 cm^{-1} , which is due to the crystalline phase. In addition, for the film deposited at a low $[\text{SiH}_4]$ of 0.1 sccm exhibits the weak broad peak at 480 cm^{-1} due to an amorphous phase. Thus, no crystallization was observed at $[\text{SiH}_4] = 0.1\text{ sccm}$, because of poor migration of deposition precursors and/or the absence of nuclear sites. Moreover, no film with the desired thickness was obtained at $[\text{SiH}_4] = 0.0\text{ sccm}$. This result means that the main precursors for film growth in this system arise from SiH_4 . The SiH_4 source gas is an attractive technique to promote the diffusivity of the deposition precursor, SiH_3 and/or the relaxation of the Si network on the H-rich growing surface.

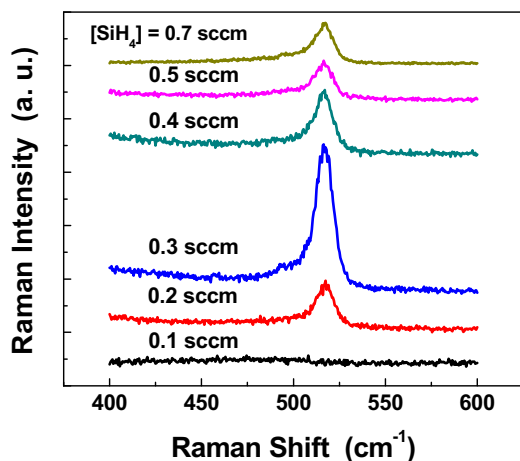


FIGURE 1. Raman spectra for nc-Si thin films with different $[\text{SiH}_4]$ values.

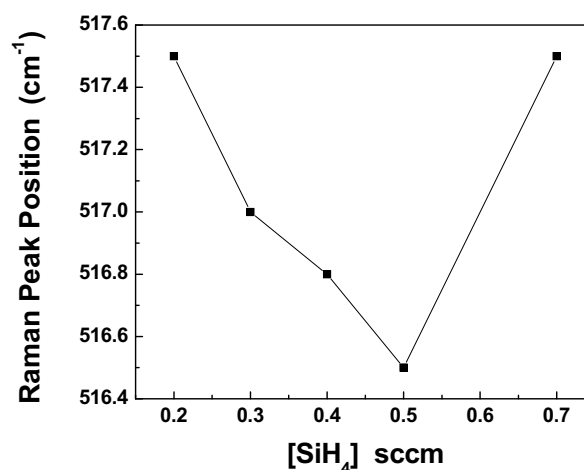


FIGURE 2. Peak frequency of the Raman signal arising from the crystalline Si phases, as a function of $[\text{SiH}_4]$, for nc-Si thin films.

As shown in Figure 1, the intensity of the 520 cm^{-1} component increases with increasing the $[\text{SiH}_4]$ up to 0.3 sccm but then decreases for $[\text{SiH}_4] > 0.3\text{ sccm}$. In addition, the peak position of TO2 changes (shifts) with increasing the $[\text{SiH}_4]$. Such Raman peak shifts would be related to a change in the stress of the films. In other words, the redshift of TO2 mode peak should be considered as the total contribution from tensile strain effect of Si nanocrystals embedded in nc-Si films. Where, a positive Raman-peak shift can be interpreted as indicating an increase in the compressive stress or a decrease in the tensile stress.

Figure 2 shows the peak frequency of the Raman signal arising from the c-Si phases of nc-Si thin films, as a function of $[\text{SiH}_4]$. As shown in Figure 2, the values of peak frequency of the Raman signal for nc-Si thin films decrease with an increase in $[\text{SiH}_4]$ up to 0.5 sccm and then rapidly increases with increasing $[\text{SiH}_4]$. A decrease of the peak frequency of the Raman signal in the range lower than 520 cm^{-1} will reflect a change in δ as stated above. The Raman shifts are controlled by vibration of the electronic polarization for constituents in the films which depends on the bonding structure such as atomic distance. On the other hand, if the atomic distance is uniformly strained, the peak frequency of Raman signal of nc-Si thin films should shifts. Such Raman peak shifts would be related to a change in the stress of the films, as mentioned above.

Figure 3 shows the XRD spectra for the nc-Si thin films deposited at different $[\text{SiH}_4]$. In these films an amorphous structure has been obtained for the film deposited at $[\text{SiH}_4] = 0.1 \text{ sccm}$, the result of this condition has not been shown here, which is consistent with the Raman results seen in Figure 1. As shown in Figure 3, the intensity of the $\langle 111 \rangle$ texture increases by increasing the $[\text{SiH}_4]$ (from 0.2 to 0.3 sccm), then decreases with $[\text{SiH}_4]$, in good agreement with the results of Raman spectra (see Figure 1). For these films we did not observe any signals due to a $\langle 110 \rangle$ and $\langle 311 \rangle$ textures. These results mean that SiH_4 plays an important role in creation of dominant $\langle 111 \rangle$ texture.

When nc-Si thin film is used as the gate electrode in a metal–oxide–semiconductor (MOS) transistor, a smooth surface is generally desired to allow patterning of small device features. However, when it is used as an electrode of the capacitor in a dynamic random-access memory (DRAM), a rough surface may be valid to increase the surface area of the capacitor. The AFM image (Figure 4) shows a homogeneous pentacene film surface with the root-mean-square (rms) roughness of 7.5 nm. As seen from Figure 4 ($[\text{SiH}_4] = 0.3 \text{ sccm}$), the shape of the grains on the surface is spherical. Furthermore, the nanocrystallites of the silicon are distributed nearly uniformly over the surface and hence are suitable for integration in device structure. It is therefore expected that grown thin films could be used as protective coatings in the device.

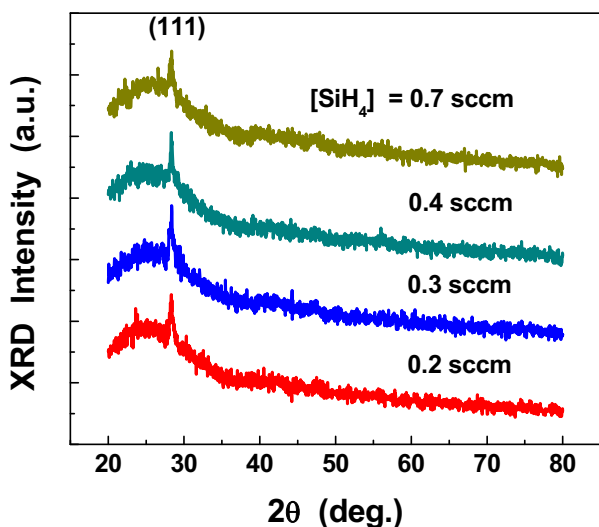


FIGURE 3. XRD spectra for nc-Si thin films with different $[\text{SiH}_4]$ values.

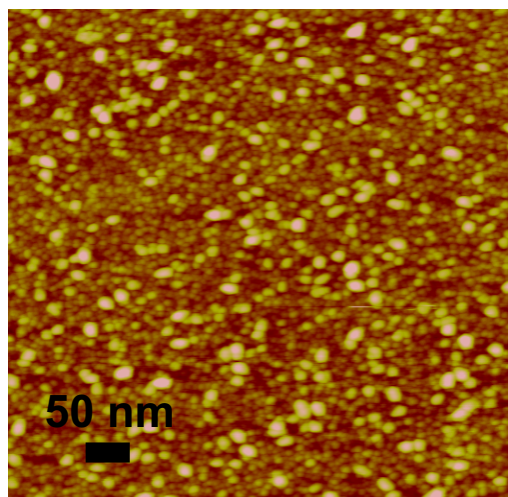


FIGURE 4. The AFM picture of deposited silicon thin films at $[\text{SiH}_4] = 0.3 \text{ sccm}$.

It is well known that when nc-Si and poly-Si are used as a gate electrode or an interconnection material in integrated circuits, the undesirable oxidation results in a limitation of its conductivity and finally can degrade circuit performance. Furthermore, the grain boundaries in the nc-Si and poly-Si, which has disordered structures including weak bonds, are expected to oxidize more rapidly than the inside of the grains with stable structure. Figure 5 illustrates the FTIR spectra over the range $400\text{--}4000 \text{ cm}^{-1}$ for several nc-Si thin films. As seen in Figure 5, the absorption bands were observed at around 2100 cm^{-1} is assigned to the dihydride, $[(\text{Si}_2)\text{--SiH}_2]$, chain structure in the

grain boundaries, or gathered (Si₃)–SiH bonds on the surface of a large void. The peaks at 900 and 630 cm⁻¹ are also the bending and rocking/wagging vibration modes of (Si₃)–SiH bonds, respectively. The stretching and bending mode of Si–O–Si vibration are also located at 1064 and 806 cm⁻¹, respectively [39,40].

The intensity of the spectra around 2100 cm⁻¹ is likely to decrease with increasing [SiH₄]. On the other hand, the Si–H stretching absorption around 2100 cm⁻¹ is not observed for the film deposited at [SiH₄] = 0.1 sccm. The density of Si–H bonds, which causes the 2100 cm⁻¹ band as stated above, monotonically decreases with increasing [SiH₄]. So, if the decrease in the density of Si–H bonds caused by increasing [SiH₄] corresponds to a reduction in the hydrogen coverage on growing surface, it is obvious that the results shown in Figure 1 are inconsistent with a model for interpreting the observation of no crystallization under high deposition temperature, T_d, proposed by Matsuda [41]. He has interpreted that no observation of crystallization phases under high T_d in terms of a decrease in the rate of the surface migration of the adsorbates, which is caused by the elimination of H atoms bonded to Si atoms on the growing surface of the film. As other role of hydrogen, H-radicals may selectively etch loosely bonded amorphous Si networks, leaving stable nanocrystals behind, and the etching effect may play an important role in growth of nc-Si thin films [32,42].

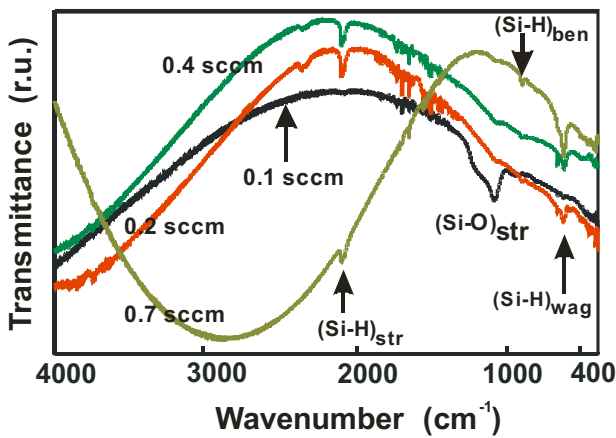


FIGURE 5. IR transmittance spectra for nc-Si thin films with different [SiH₄] values.

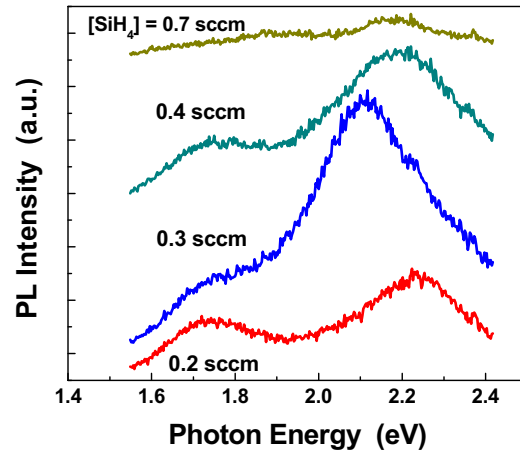


FIGURE 6. Photoluminescence (PL) spectra for nc-Si thin films with different [SiH₄] values.

Figure 6 shows the PL spectra for four different films with [SiH₄] = 0.2, 0.3, 0.4 and 0.7 sccm. The PL spectra showed four peaks at around 2.28-2.38, 2.19-2.25, 2.0-2.1, and 1.77-1.8 eV at room temperature, respectively. These PL peak energies values were found in an energy range higher than the band gap energy for c-Si (1.12 eV). This result may be interpreted in terms of a model that grains with smaller δ preferentially exit in shallower layer of the films depending on the growth of mechanism of the films. This is because excitation and absorption process in the PL will occur in the side of the free surface that light was irradiated. In addition, no PL is observed for the film deposited at [SiH₄] = 0.1 sccm, which was amorphous as seen in Figure 1. Therefore, it is considered that an amorphous Si phase is not responsible for the observed luminescence in the present work. Trwoga et al. [43] examined the effects of changing both the mean grain size and the size distribution for grains with a nanometer scale on the width and the peak energy of the PL spectra, utilizing the effective mass approximation. In that work, they showed that the PL spectra exhibited blueshifts and broadening as the mean grain size decreased. Furthermore, they showed that the oscillator strength rapidly increased with decreasing average size. Edelberg et al. [26] have examined the origins of the band approximately 2.0–2.1 eV. One of the origins may be due to defects related to oxygen [44]. Another origin may be associated with SiH- related bonds [45]. In the present work, the decrease in the density of Si–H bonds with increasing [SiH₄] (figure 5) corresponds with the decrease in the 1.77-1.8 PL band (figure 6), similar relationship was found by Umezū et al. [46] for a-Si:H prepared by rf sputtering at higher temperature. Thus, the results shown in figure 5 and figure 6 indicate that the contribution of SiH-related bonds on

the PL spectra cannot be excluded. On the other hand, the spectra around 2.0 - 2.4 eV may arise from small grains (quantum size effect). In addition, to know the exactly origin of PL, another measurements are needed.

CONCLUSION

Nanocrystalline silicon (ns-Si) thin films with different silane flow rates ($[\text{SiH}_4]$) have been prepared using plasma-enhanced chemical vapor deposition technique. No crystalline phase was observed at $[\text{SiH}_4] = 0.1$ sccm. As a result of the photoluminescence (PL) and the infrared (IR) absorption measurements, the decrease in the density of Si-H bonds with increasing $[\text{SiH}_4]$ was found to correspond with the decrease in the 1.77 - 1.8 eV PL band. On the other hand, the 2.0 - 2.4 eV PL band may be due to nanocrystals in the films. Furthermore, we have shown that a structural change from amorphous to nanocrystalline easily occurs with increasing $[\text{SiH}_4]$.

ACKNOWLEDGEMENTS

This work is kindly supported by King Abdulaziz City for Science and Technology (Contract number: 08-NAN153-7).

REFERENCES

1. L.T. Canham, Appl. Phys. Lett. 57 (1990) 1046.
2. S. Guha, J. Yang, D.L. Williamson, Y. Lubianiker, J.D. Cohen, A.H. Mahan, Appl. Phys. Lett. 74 (1999) 1860.
3. J.-H. Shim, S. Im, N.-H. Cho, Appl. Surf. Sci. 234 (2004) 268.
4. S. Furukawa, T. Miyasato, Phys. Rev. B 38 (1988) 5726.
5. H. Takagi, H. Ogawa, Y. Yamazaki, A. Ishizaki, T. Nakakiri, Appl. Phys. Lett. 56 (1990) 2379.
6. H.C. Cheng, C.Y. Huang, F.S. Wang, K.H. Lin, F.G. Tarntair, Jpn. J. Appl. Phys. 39 (2000) L19.
7. T.E. Dyer, J.M. Marshall, W. Pickin, A.R. Hepburn, J.F. Davies, J. Non-Cryst. Solids 164-166 (1993) 1001.
8. A.G. Aberle, N.P. Harden, S. Oelting, J. Cryst. Growth 226 (2001) 209.
9. A.M. Ali, T. Inokuma, Y. Kurata, S. Hasegawa, Jpn. J. Appl. Phys. 38 (1999) 6047.
10. Y. Nasuno, M. Kondo, A. Matsuda, Jpn. J. Appl. Phys. 41 (2002) 5912.
11. J.-H. Shim, S. Im, N.-H. Cho, Appl. Surf. Sci. 234 (2004) 268.
12. H. Chen, W.Z. Shen, Surf. Coat. Tech. 198 (2005) 98.
13. X.X. Wang, J.G. Zhang, L. Ding, B.W. Cheng, W.K. Ge, J.Z. Yu, Q.M. Wang, Phys. Rev. B 72 (2005) 195313.
14. A.M. Funde, N.A. Bakr, D.K. Kamble, R.R. Hawaldar, D.P. Amalnerkar, S.R. Jadhkar, Solar Energy Mater. & Solar Cells 92 (2008) 1217.
15. A. Shah, J. Meier, E. Vallat-Sauvain, C. Droz, U. Kroll, N. Wyrsch, J. Guillet, U. Graf, Thin Solid Films 403-404 (2002) 179.
16. A. Tanaka, G. Yamahata, Y. Tsuchiya, K. Usami, H. Mizuta, S. Oda, Cur. Appl. Phys. 6 (2006) 344.
17. H.L. Hsiao, H.L. Hwang, A.B. Yang, L.W. Chen, T.R. Yew T.R., Appl. Surf. Sci. 142 (1999) 316.
18. B.A. Scott, R.M. Plecenik, E. Esimonyi, W. Reuter, Appl. Phys. Lett. 40 (1982) 973.
19. S. Binetti, M. Acciarri, M. Bollani, L. Fumagalli, H. von Kanel, S. Pizzini, Thin Solid Films 487 (2005) 19.
20. M. Acciarri, S. Binetti, M. Bollani, A. Comotti, L. Fumagalli, S. Pizzini, H. Von Kanel, Solar Energy Mater. & Solar Cells 87 (2005) 11.
21. M. Modreanu, E. Aperathitis, M. Androulidaki, M. Audier, O.-C. Pluchery, Opt. Mater. 27 (2005) 1020.
22. M. Fonrodonaa, D. Solera, J. Escarrea, F. Villara, J. Bertomeua, J. Andreua, A. Saboundjib, N. Coulonb, T.M. -Brahimb, Thin Solid Films 501 (2006) 303.
23. R. Saleh, N.H. Nickel, Thin Solid Films 427 (2003) 266.
24. S. Veprek, T. Wirschem, M. Ruckschloß, H. Tamura, J. Oswald, Mater. Res. Soc. Symp. Proc. 358 (1995) 99.
25. G. Cicala, G. Bruno, P. Capezzuto, L. Schiavulli, V. Capozzi, G. Perna, Mater. Res. Soc. Symp. Proc. 452 (1997) 809.
26. E. Edelberg, S. Bergh, R. Naone, M. Hall, E.S. Aydil, J. Appl. Phys. 81 (1997) 2410.
27. J.H. Kim, K.A. Jeon, G.H. Kim, S.Y. Lee, Opt. Mater. 27 (2005) 991.
28. A.M. Ali, J. Luminescence 126 (2007) 614.
29. D. Milovzorov, T. Inokuma, Y. Kurata, S. Hasegawa, J. Electrochem. Soc. 145 (1998) 3615.
30. S.K. Kim, K.C. Park, J. Jang, J. Appl. Phys. 77 (1995) 5115.
31. H.J. Lim, B.Y. Ryu, J.I. Ryu, J. Jang, Thin Solid Films 289 (1996) 227.
32. I. Solomon, B. Drevillon, H. Shirai, N. Layadi, J. Non-Cryst. Solids 164-166 (1993) 989.
33. S. Oda, M. Odobe, Mater. Res. Soc. Symp. Proc. 358 (1995) 721.
34. K. Shimakawa, J. Non-Cryst. Solids 266-269 (2000) 223.
35. R. Carius, J. Muller, F. Finger, N. Harder and P. Hapke, *Thin Film Materials and Devices*, World Scientific, Singapore (1999) p. 157.

36. A.D. Nocera, A. Mittiga, A. Rubini, *J. Appl. Phys.* 78 (1995) 3955.
37. F. Liu, M. Zhu, Y. Feng, Y. Han, J. Liu, *Thin Solid Films* 395 (2001) 97.
38. W. Wei, G. Xu, J. Wang, T. Wang, *Vacuum* 81 (2007) 656.
39. D.V. Tsu, G. Lucovsky, B.N. Davidson, *Phys. Rev. B* 40 (1989) 1795.
40. A. Singh, *J. Non-Cryst. Solids* 122 (1990) 223.
41. A. Matsuda, *J. Non-Cryst. Solids* 59/60 (1983) 767.
42. S. Kumar, B. Brevillon and C. Godet, *J. Appl. Phys.* 60 (1986) 1542.
43. P. F. Trwoga, A. J. Kenyon and C. W. Pitt, *J. Appl. Phys.* 83 (1998) 3789.
44. A.J. Kenyon, P.F. Trwoga and C.W. Pitt, *J. Appl. Phys.* 79 (1996) 9291.
45. X. Zhao, O. Schoenfeld, J. Kusano, Y. Aoyagi and T. Sugano, *Jpn. J. Appl. Phys.* 33 (1994) L649.
46. I. Umezu, K. Yoshida, N. Sakamoto, T. Murota, Y. Takashima, M. Inada and A. Sugimura, *J. Appl. Phys.* 91 (2002) 2009.